Potential of Wave Energy Harvesting in the North Sea; The AE-Wave Hexapod WEC

JH Paulides, Johannes; Rajita Shenoi, R.; Van Bodegraven, Frank; Nijman, Lucas; Jonkman, Remi; Encica, Laurentiu; Wellens, Peter

DOI
10.1109/TMAG.2024.3413289

Publication date
2024

Document Version
Final published version

Published in
IEEE Transactions on Magnetics

Potential of Wave Energy Harvesting in the North Sea; the AE-Wave Hexapod WEC

Johannes J. H. Paulides [1,2], R. Rajita Shenoi [2], Frank van Bodegraven [2], Lucas Nijman [2], Remi Jonkman [1], Laurentiu Encica [1], and Peter Wellens [3]

[1]Advanced Electromagnetics Group, 5161 EA Waalwijk, The Netherlands
[2]AE-Wave Hexapod, 3316 AX Dordrecht, The Netherlands
[3]Ship Hydromechanics and Structures, Delft University of Technology, 2628 CD Delft, The Netherlands

Energy from ocean surface waves is the most prominent form of marine energy. The waves are produced by gravitational water waves (2.2e^{-5} Hz), in combination with the short wind and swell waves (0.03−1 Hz). The energy density and predictability of waves make them an extremely interesting form of sustainable energy. Wave energy is therefore an ideal addition to the energy mix. Research has confirmed that (part) synergy is possible with offshore wind farms because the energy production profile over time of wave energy (even on a relatively sheltered inland North Sea) is not synchronous with the energy profile of wind, mainly due to swell waves and therefore is, at least, partly complementary to that of offshore wind. Wave energy can be generated via so-called wave energy converters (WECs). This article describes the potential of an innovative WEC with existing regenerative robots to be used in energy harvesting in the North Sea.

Index Terms— **Assembly robots, energy conversion, offshore distribution systems, wave energy conversion, wind energy solar.**

I. Introduction

WAVE energy is an essential addition to the energy mix to contribute to the Dutch and European climate goals of reducing net emissions by 55% by 2030 and becoming the climate-neutral continent by 2050. The synergy of wave energy converters (WECs) is possible with offshore wind farms and large-scale deployment of floating solar arrays. This is due to the fact that the energy production profile of wave energy does not, perfectly, align with those of wind and solar energy which are partly complementary [1]. Waves are variable by nature and wave energy is therefore also variable. Wave energy lags behind wind strength by about half a day, so energy can still be produced after the wind dies down. Wave energy can thus supplement offshore wind and dampen the variability of electricity supply from the sea. Existing WECs can generate significant amounts of energy only with large wave motions, and mainly do so only in a single dimension. In contrast, the Wave Hexapod (WHP) can generate energy very efficiently in all three dimensions even with small wave motions. The WHP has six (hexa) robots as legs on three buoys that can directly generate energy. Regenerative robots were chosen to use existing technology and, therefore, scale up faster. The design features of the WHP, the available energy for power extraction at the North Sea, the design of buoys for maximum energy absorption and the integration of such WECs into a standard offshore wind energy platform are described in this article.

II. Working Principle WHP

The WHP can be attached to a floating body (tri-floater as an energy island as shown in Fig. 1), a wind turbine, or an oil rig, and looks like a three-legged spider with three floating buoys attached to its legs. Six energy-generating ABB 7600 robots, two per leg of the spider, form the intelligent and freely programmable heart of the WHP. These robots are attached by a steel structure to the three floating buoys. The buoys constantly follow the movement of the waves and by sort of slowing them down with the robot, the six robots generate energy. The robots, which in a previous life were used to assemble cars, can follow any, i.e., even high frequency, wave shapes, allowing us to extract energy from all three dimensions of the wave spectrum. Another advantage is that the robots, which we are giving a second life, can be obtained in thousands. So these generating robots are already suitable for high-volume applications.

The patented innovative aspect is that the WHP uses the robot joint motors not as “motors” but as “multi-dimensional generators.” Mechanical energy is supplied to the robots that are gravitationally compensated and electrical energy is extracted from the generators that are present in the robot joints. The WHP can be connected to the existing infrastructure in the sea, to which wind turbines are also connected. The WHP collects the energy and brings it to a large “shared socket.” From there, the energy can go to land. Via a special construction, the WHP can be hoisted above the water, e.g., when the waves are too high, for maintenance or when sufficient energy is already being generated by wind turbines or offshore solar.

III. Available Power in the North Sea

The North Sea is an inland sea located between the Western European continent, the Scandinavian Peninsula, and the U.K. with an average depth of 94 m. Availability of power at a location in turn determines the maximum power that can be extracted using a WEC. The available average annual wave power ranges from approximately 5.5 to 10 kW/m for

Manuscript received 24 March 2024; revised 6 June 2024; accepted 6 June 2024. Date of publication 12 June 2024; date of current version 27 August 2024. Corresponding author: J. J. H. Paulides (e-mail: johan@ae-grp.nl).

Color versions of one or more figures in this article are available at https://doi.org/10.1109/TMAG.2024.3413289.

Digital Object Identifier 10.1109/TMAG.2024.3413289

Fig. 1. WHP as part of Energy Island, containing "Small" Wind Turbine (ca. 4GWh per year), Solar (ca. 1.8 MWh per year), Wave (ca. 5.5 GWh), Battery (ca. 30 MWh), Electrolyzer, and Fuelcell to guarantee 1 MW to be supplied 24/7 for 365 days per year.

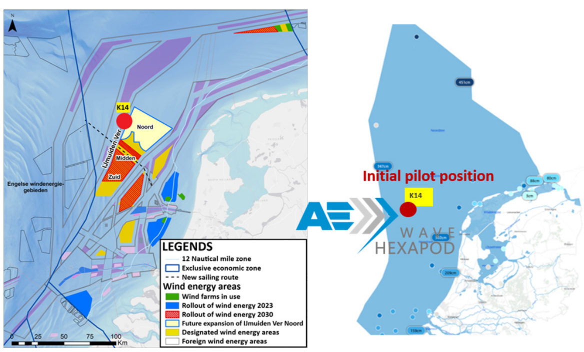

Fig. 2. K14 location within the North Sea from which the data has been collected.

7.5 and 30 km offshore from the Dutch continental shelf, respectively [2].

To calculate the power available at a potential location (K14 platform) in the North Sea, the following method was adopted. The significant wave height and the peak wave period are parameters that define wave conditions in a particular area. It is defined as the average height of the highest one third of the waves and wave period with the most energy in the given wave dataset, respectively. Data of measured free surface elevations until the end of 2020 was collected for the K14 platform near the Dutch coast from [3]. The K14 is within the large wind turbine parks as currently present in the North Sea part of the Netherlands, as shown in Fig. 2. The WHP can be integrated into the offshore power platform using the electrical infrastructure and supplying energy to the power grid on shore (Fig. 3).

The collected data were converted into a joint probability diagram of significant wave height and peak period ("scatter diagram"), in which the wave height was binned in 1 m increments and the peak period was binned in 2 s increments. The available mean wave power was determined for each

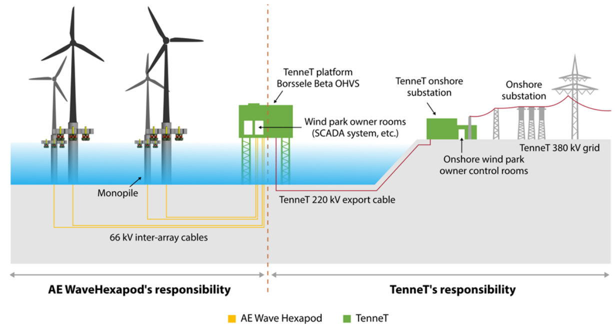

Fig. 3. Simplified system overview in case the WHP is directly connected to a Wind Turbine and uses the same electrical infrastructure to transport the energy to the shore.

combination of significant wave height and peak period as follows:

$$\overline{P} = \int_0^\infty E c_g d\omega \tag{1}$$

with $\overline{P}$ is the mean power, E is the Energy in a wave component, c_g is the component's group velocity, and ω is the radial frequency. The yearly mean of available mean wave power was then determined as the average of mean power per wave spectrum, weighted with the relative occurrence of that wave spectrum. According to this calculation, the average of mean wave power is 13 kW/m crest length.

Alternatively, the time-averaged power from irregular waves can be calculated using the following equation [4]:

$$P_w = \frac{\rho g^2}{64\pi} H_s^2 T_e \tag{2}$$

where P_w is the power per meter wave crest in kW/m, T_e is the wave energy period in seconds, and H_s is the significant wave height in m. The wave energy period can be estimated from the peak wave period using the following equation:

$$T_e = \frac{T_p}{1.12}. \tag{3}$$

The environmental data for the year 2022 was collected [3] and the occurrences have been plotted in a scatter diagram as given in Fig. 4. The power available for energy harvest weighted with occurrence is shown in Fig. 5. Around 90% of occurrences fall within the significant wave height range from 0.25 to 2.25 m, with the peak wave period ranging between 3.2 and 12 s. Analysis of the power scatter diagram reveals that the power available for maximum energy harvest occurs at 2.25 m and 7.1 s. The majority of power that is available, weighted with occurrence, is of the wave height below 5 m. The average mean wave power available is 16 kW/m. This data must be considered when designing WECs for a specific region in the North Sea. The device must be able to capture energy at lower ranges of the significant wave height and the peak wave period compared to energy-rich areas around the world.

IV. Buoy Design

The shape, size, and geometry of the buoy are critical factors that influence the power absorption capability of a WEC. Hence, developing a suitable buoy model is an essential task in the WEC design. A vertical cylindrical buoy with a

Occurrences (%) Sign. Wave Height, Hs(m)	Peak Wave Period, Tp (s) 0.6	1.9	3.2	4.5	5.8	7.1	8.4	9.7	11	12.3	13.5	14.8	16.1	17.4	18.7	20	21.3	22.6	23.9	25.2	26.4	Total (%)
0.25			1.9	4.4	2.9	1.7	0.8	0.4	0.4	0.4	0.2	0.01									0.002	13.1
0.75			1.6	10.1	9.1	4.6	2.2	1.5	0.3	0.03	0.04	0.01	0.01	0.02	0.01							29.5
1.25				3.2	11.7	5.4	3.1	1.1	0.6	0.2	0.09	0.08	0.03	0.03	0.01							25.5
1.75				0.04	4.5	4.9	1.7	0.8	0.3	0.09	0.02	0.01	0.01	0.01			0.002					12.3
2.25					0.7	5.4	1.6	0.7	0.4	0.07	0.06	0.02							0.002			8.9
2.75					0.02	2.5	1.9	0.4	0.2	0.08	0.02	0.01	0.002						0.002			5.1
3.25						0.3	1.4	0.5	0.2	0.1	0.04	0.002										2.5
3.75						0.01	0.7	0.4	0.2	0.05	0.05	0.03	0.01	0.002								1.4
4.25							0.1	0.2	0.3	0.07	0.03	0.02	0.02									0.8
4.75							0.03	0.2	0.2	0.09	0.07	0.02	0.01									0.6
5.25							0.002	0.09	0.08	0.02	0.03	0.02	0.004									0.3
5.75								0.02	0.03	0.03		0.002										0.08
6.25								0.002	0.05	0.01	0.01		0.002									0.07
6.75								0.004	0.02	0.02												0.04
7.25									0.01	0.002	0.004											0.01
7.75									0.004													0.000
																						100

Fig. 4. Occurrence data of wave parameters at the K14 platform for 2022.

$P_{available}$ weighted with occurrence Sign. Wave Height, Hs(m)	Peak Wave Period, Tp (s) 0.6	1.9	3.2	4.5	5.8	7.1	8.4	9.7	11	12.3	13.5	14.8	16.1	17.4	18.7	20	21.3	22.6	23.9	25.2	26.4	Average weighted Pavailable (kW/m)
0.25			1.6	5.5	4.6	3.3	1.9	1.1	1.3	1.3	0.7	0.0									0.01	0.5
0.75			13.0	112.4	129.9	80.1	44.5	35.2	7.9	0.9	1.2	0.5	0.3	0.7	0.4							28.6
1.25				98.9	464.2	260.6	175.4	75.4	42.2	15.9	8.0	8.4	3.8	3.2	0.7							78.0
1.75				2.5	350.9	462.7	190.0	100.3	41.6	14.1	3.8	2.7	2.5	3.1			0.6					42.5
2.25					83.7	847.4	298.4	158.4	90.2	17.7	18.4	6.3							1.0			52.5
2.75					3.3	584.8	526.5	120.8	63.9	33.4	8.6	6.6	1.0						1.5			25.1
3.25						93.5	533.5	225.2	80.5	72.7	26.4	1.3										9.0
3.75						5.0	357.6	210.9	130.5	36.1	44.7	26.2	5.7	2.05								3.5
4.25							71.1	190.3	227.3	70.5	32.8	26.9	19.5									1.2
4.75							22.2	184.7	182.4	104.2	94.7	33.6	18.3									0.8
5.25							1.9	100.5	103.8	36.8	56.3	44.5	7.5									0.2
5.75								21.4	51.6	57.7		4.1										0.04
6.25								3.2	89.7	28.1	13.3		5.3									0.05
6.75								7.4	46.0	37.4												0.02
7.25									14.5	5.4	11.9											0.001
7.75									11.0													0.0004
																					Average $P_{available}$ (kW/m)	16

Fig. 5. Available power weighted with occurrence for the K14 platform.

large draft and radius has enhanced energy absorption since the hydrostatic parameter added mass is high. However, this leads to an increased volume, resulting in reduced damping and increased buoy mass. Considering these aspects, a three-sectioned buoy based on [5] is developed for the AE WHP. Salient dimensions which have been varied for optimizing the buoy design are marked in Fig. 6 and the corresponding data has been given in Table I.

The objective is an optimized buoy design by enhancing the frequency-dependent parameters. For this, added mass and radiation damping must be as high as physically possible. Therefore, the top portion of the buoy is made as wide as possible at the free surface so that the buoy has a good absorption width for the incoming waves. Draft, the underwater cross-sectional area of the buoy, has a critical influence on the radiation damping and it needs to be optimized. When the draft increases, radiation damping amplitude decreases narrowing the bandwidth of the WEC. The middle cylindrical section is optimized in length and diameter so that the draft is minimized while at the same time, sufficient structural support is maintained. The shape and size of the third section of the buoy adds inertia to the oscillating system which helps to adjust the natural frequency to match the dominant incident wave. The bottom section is designed to avoid sharp corners, preventing the formation of eddies from fluid flow around it, which could adversely affect the buoy's performance. In addition to evaluating frequency-dependent parameters, the power absorbed by the buoy under North Sea environmental conditions is also assessed for different parametric designs.

The power absorbed by a WEC depends on the forces acting on the buoys. In this study, these forces are estimated by performing numerical simulations using ANSYS AQWA, a potential theory-based hydrodynamic analysis software that determines environmental loads on fixed or floating marine structures. It utilizes the source distribution method to compute

TABLE I

BUOY CHARACTERISTICS

Parameter	Description	Value
R_T	Radius of top section (m)	6
L_T	Total Length (m)	10
d	Draft (m)	9.05
R_B	Radius of bottom section (m)	3.2
L_B	Length of bottom section (m)	2.1
M	Mass (kg)	20,000

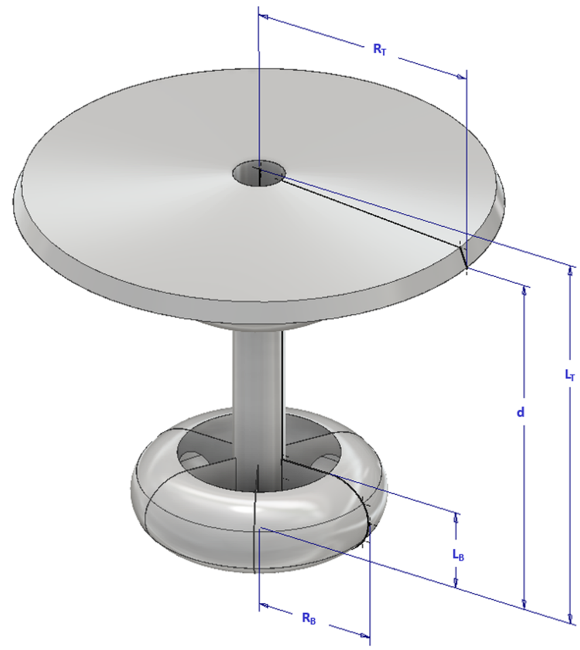

Fig. 6. AE WHP buoy geometry.

velocity potentials and fluid pressure around submerged structures [6].

This simulation model using ANSYS AQWA is first verified by comparing the hydrodynamic diffraction analysis results using the geometric model presented in [5]. The comparison shows consistent trends for all frequency-dependent parameters as illustrated in Fig. 7. The results for radiation damping and excitation forces reasonably agree with the literature [5], though there are discrepancies in the added mass. These discrepancies may be due to a lack of clarity in the geometric and other characteristic buoy data in [5]. The study in [5] presents optimized parametric values for the main geometry within a range of values, and median values were assumed in the present analysis. Some specific dimensions of the geometry were unavailable, so suitable values were assumed. These differences led to variations in the buoy's volume, which subsequently affected the mass of fluid displaced by the buoy, impacting the calculation of added mass.

The buoy geometry design (Fig. 6) is modeled in CAD software, AUTODESK INVENTOR, and then imported to ANSYS AQWA. A water depth of 25 m and density of 1025 kg/m^3 is considered for the analysis.

Ocean waves are irregular in nature. The sea state for irregular waves used in the study was the Joint North Sea Wave Project (JONSWAP) which has significant wave height and peak wave period to describe the spectrum. This is a reasonable representation of the whole spectrum of sea states

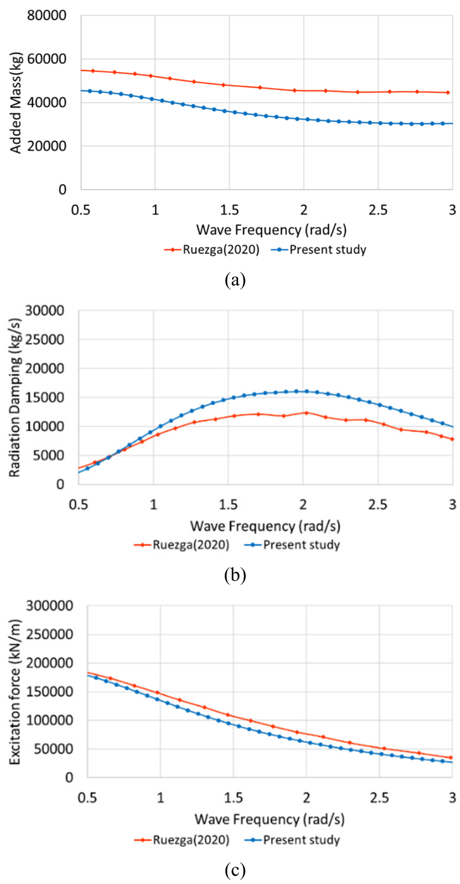

Fig. 7. Hydrodynamic coefficients from simulations such as (a) added mass, (b) radiation damping, and (c) excitation force.

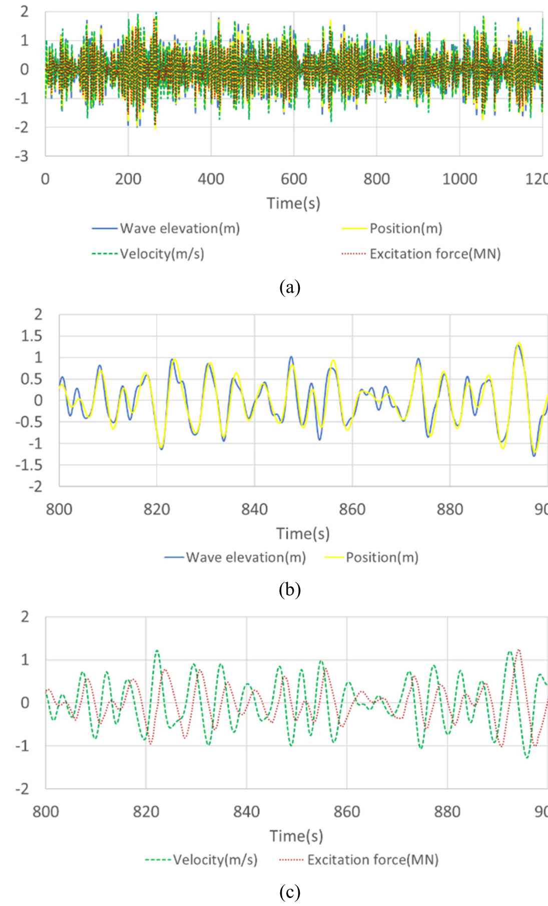

Fig. 8. Simulation results of irregular waves with a peak period of 7.1 s and significant wave height of 2.5 m. (a) Overview of the results. (b) Part of upper image depicting wave elevation and buoy position. (c) Part of upper image showing velocity and excitation force.

Power absorbed by AE Wave hexapod	Peak Wave Period, Tp (s)																					Total percentage weighted with occurrence (%)
Sign. Wave Height, Hs(m)	0.6	1.9	3.2	4.5	5.8	7.1	8.4	9.7	11	12.3	13.5	14.8	16.1	17.4	18.7	20	21.3	22.6	23.9	25.2	26.4	
0.25			0.4	0.6	0.7	0.9	1.0	1.2	1.4	1.5	1.7	1.8										1
0.75			3.6	5.0	6.4	7.9	9.3	10.7	12.2	13.6	15.0	16.5	17.9	19.3	20.7							7
1.25				13.9	17.9	21.9	25.8	29.8	33.8	37.8	41.7	45.7	49.7	53.7	57.6							20
1.75				27.3	35.1	42.8	50.6	58.4	66.2	74.0	81.8	89.6	97.4	100			96.4					43
2.25					58.0	70.8	83.7	96.6	100	100	100	100							100			76
2.75					50.6	61.9	73.1	84.4	95.6	100	100	100	100						100			70
3.25						86.4	100	100	100	100	100	100										98
3.75						80.4	95.0	100	100	100	100	100	100	100								97
4.25							100	100	100	100	100	100	100									100
4.75							100	100	100	100	100	100	100									100
																					Average percentage (%)	54

Fig. 9. Power matrix of the AE WHP.

encountered in the North Sea. Fig. 8(a) shows the simulation result of an irregular wave spectrum using JONSWAP with a peak period of 7.1 s and a significant wave height of 2.25 m. Fig. 8(b) shows part of the simulation comparing wave elevation and position of the buoy with respect to it. It is evident that in the absence of any additional damping, the buoy moves with the waves. Fig. 8(c) shows the part of the time series of velocity and excitation force. The optimum condition for power absorption occurs when velocity is in phase with the excitation force of the incident waves.

Due to the limitation of time and resources a select number of significant simulations were carried out, highlighted by black-bordered cells in Fig. 5. The corresponding significant wave height and peak wave period are denoted in red font color.

The simulation results are extrapolated to other environmental conditions to generate the scatter diagram of absorbed power. The power matrix in terms of the percentage of full capacity (rated power) considering the three buoys of the AE WHP is generated as shown in Fig. 9. Note that the working limit of the AE WHP is wave heights lesser than 5 m. It works in full capacity for wave heights higher than 1.75 m and is able to capture 70% of the maximum power available at 2.25 m and 7.1 s. The average efficiency of the AE WHP excluding the power take off (PTO) mechanism is approximately 54%.

V. Hybrid Wind-Wave Power

There is, of course, a correlation between wind and wave energy because in the North Sea wave energy is mainly wind driven. However, even in the North Sea, the generation of wave energy lags a few hours behind the generation of wind energy! Therefore, the wave energy continues to be produced for a while even after the wind stops. Thus, from a hybrid offshore energy platform, this phenomenon will result in the continuous and/or increased generation of power at moments when the wind is less present [7]. There are also instances where there are inverse correlations during specific times of the day or short periods. Energy sources on a typical winter, spring, summer, and autumn day at the K14 platform are given in Fig. 10.

Four submersibles, each carrying six AE WHPs can produce about 15 MW of power at full capacity. This is equivalent to an offshore energy platform with a 15 MW wind turbine (Fig. 11). The power from multiple WHPs on submersibles

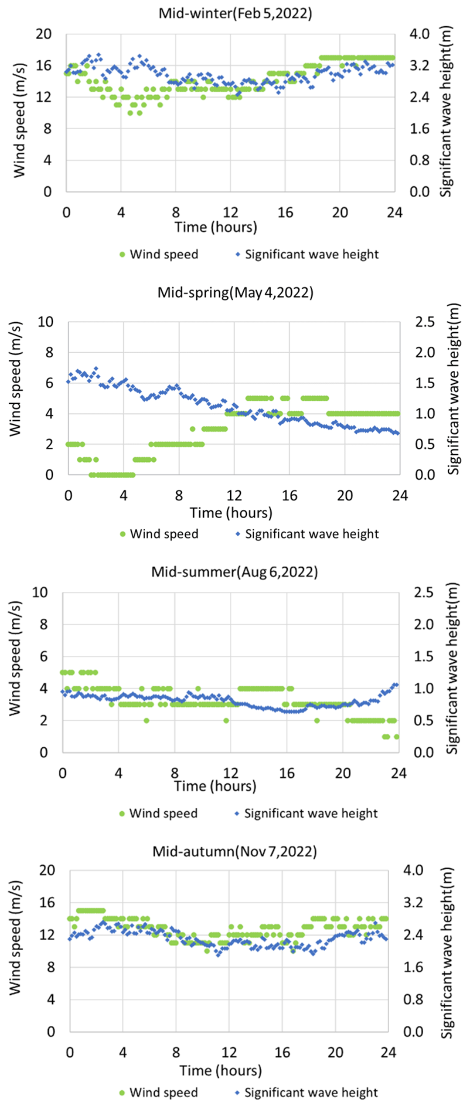

Fig. 10. Seasonal correlation per 24 h for a specific day of wind speeds and significant wave heights in a year.

Fig. 11. Hybrid power platform-15 MW wind turbine with 6 AE WHPs on each of the 4 semisubmersibles.

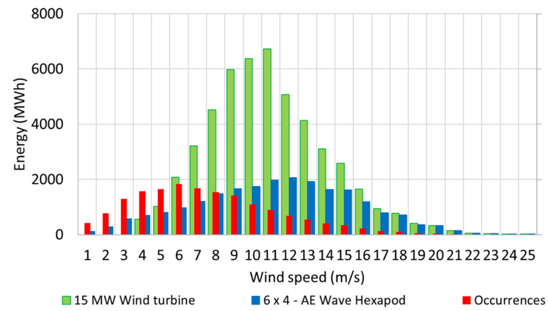

Fig. 12. Energy (MWh) versus wind speed (m/s) curves of the hybrid power platform consisting of 15 MW wind turbine and 24 AE WHPs with occurrences of wind speed in hours incorporated.

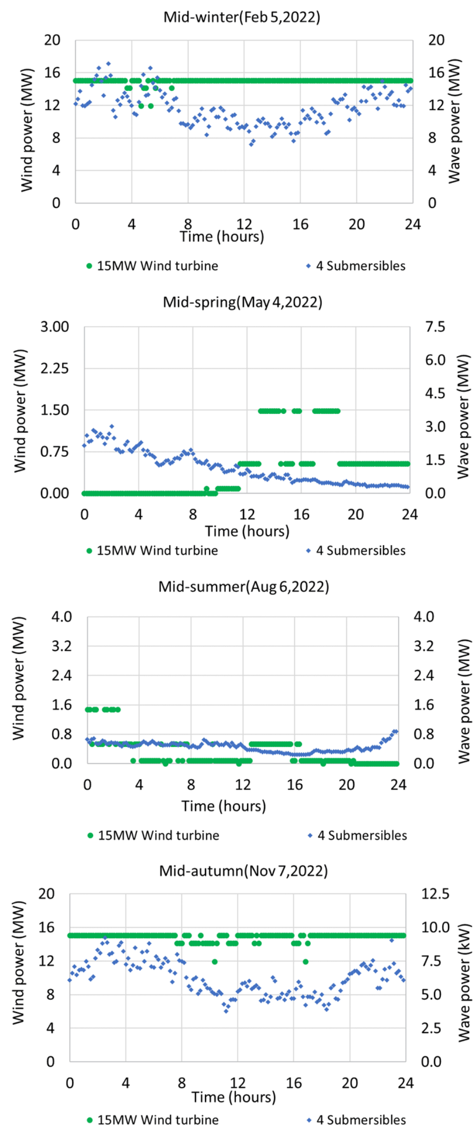

Fig. 13. Seasonal correlation per 24 h for a specific day of wind and wave energy extracted from a 15 MW wind turbine and equally rated four submersibles of 6 AE WHPs.

is an alternate or complementary source of power from an offshore energy platform.

To evaluate the hybridization of the AE WHP with a 15 MW wind turbine, the power generated by both systems over the course of one year (2022) is estimated for given the environmental conditions. The average power from the 15 MW wind turbine corresponding to the wind speeds occurring throughout the year is estimated using the data from the power curve [8]. The wave height and wave period data for the corresponding wind speed are estimated to calculate the average power output from AE WHP. The absorbed power from the AE WHP and the 15 MW wind turbine is plotted

TABLE II
SEASONAL AVERAGES

Seasons of 2022	Wind speed (m/s)	Wave height (m)	Wave period (s)	Wind turbine power (MW)	Total Wave power (MW)	Total hybrid power (MW)
Winter	9.42	1.78	6.44	8.70	4.44	13.06
Spring	6.55	1.04	4.87	4.83	1.51	6.30
Summer	5.81	0.96	4.70	3.51	1.27	4.75
Autumn	8.61	1.56	6.02	7.55	3.40	10.94

against the wind speeds. The occurrences of wind speeds over the year are also incorporated in the graph (Fig. 12). The wind speeds (<11 m/s) when a wind turbine does not run at full capacity occur about 80% of the total time in a year. It can be seen that the AE WHP does contribute power to the offshore energy platform especially at lower wind speeds when the wind turbine is running below full capacity. On average, the AE WHP contributes an additional 9% of power to the total energy production from the offshore energy platform when wind speeds are less than 11 m/s. At wind speeds lesser than cut in speed where there is no power generation by the wind turbine, the AE WHP solely contributes to about 15% of the total capacity from the platform.

The correlation between wind and wave energy at different seasons gives information about the expected energy distribution from a hybrid platform throughout the year. Power generation from such a hybrid platform with a 15 MW wind turbine and four submersibles each with six AE WHPs on typical days in every season in the year 2022 at the K14 platform is given in Fig. 13. Data shows that indeed the wave energy does aid the energy mix at various times within a certain day. This is in particular seen on the spring and summer days when the wave energy provides useful addition, considering the fact that the wind turbine does not run at full capacity during these periods.

The averaged data estimated for various parameters during the seasonal periods in a year are summarized in Table II. The contribution of wave power to the hybrid platform is quite significant and does point toward its viability.

VI. CONCLUSION

The available power for energy harvesting weighted with occurrences at the K14 platform in the North Sea is generated for the year 2022. An average mean wave power of 16 kW/m is available. About 90% of the data instances fall within the significant wave height range from 0.25 to 2.25 m and peak wave period range from 3.2 to 12 s. The maximum energy is available at a significant wave height of 2.25 m and a peak wave period of 7.1 s. It shows that even in the relatively sheltered inland North Sea wave energy is still a suitable addition to the energy mix, since it is complementary to wind.

Buoy design plays a crucial role in energy extraction in a WEC for a certain location. Also, buoy design is emphasized to maximize the conversion efficiency from wave to electricity. A three-sectioned buoy is developed and optimized with an emphasis on enhancing the frequency-dependent parameters such as added mass and radiation damping. Numerical simulations using ANSYS AQWA are simulated to estimate power absorbed for different environmental conditions. The average efficiency of the AE WHP, excluding the PTO mechanism, is approximately 54%.

Hybridization of the offshore wind energy platform using multiple AE WHPs on submersibles is studied. The correlation between the wind and wave energy is close, whereas in wave energy generation lagging, a few hours behind wind energy generation. From the data analysis of 2022, there are instances of inverse correlation, especially in the spring and summer seasons, where the WHP can contribute positively to power generation. The specific power characteristics for both the selected wind turbine and the WHP are studied. Four submersibles, each carrying six AE WHPs can produce about 15 MW of power at full capacity and thus provide an alternate or complementary source of power to the energy platform. From the power curves for the 15 MW wind turbine and AE WHPs, it can be seen that the contribution to power generation from the AE WHPs is significant at lower wind speeds when the wind turbine operates below full capacity.

Four submersibles each carrying six AE WHPs (without wind turbine, etc) generate 23.7 GWh at the K14 location with wind speeds <11 m/s. Actually considering the no- or too little wind conditions, these WHPs still provide 9.57 GWh of energy to an offshore 15 MW monopole-based wind turbine. Furthermore, at wind speeds below the cut-in speed where the wind turbine does not generate power, the AE WHP already contributes about 0.98 GWh to the energy platform with the wind turbine.

A single submersible with six AE WHPs as part of Energy Island, containing “Small” 1.2 MW Wind Turbine (ca. 4 GWh per year), Solar (ca. 1.8 MWh per year), Wave (ca. 5.5 GWh), Battery (ca. 30 MWh), Electrolyser, and Fuel cell is able to guarantee 1 MW to be supplied 24/7 for 365 days per year.

REFERENCES

[1] S. Lamboo and R. van den Brink, “Stroom uit water,” TNO, Amsterdam, The Netherlands, Tech. Rep. TNO 2020 P11977, 2021.

[2] C. Beels, J. C. C. Henriques, J. De Rouck, M. T. Pontes, G. De Backer, and H. Verhaeghe, “Wave energy resource in the North Sea,” in *Proc. 7th EWTEC*, 2007, pp. 1–10, doi: 10.13140/2.1.4640.6403.

[3] *Rijkswaterstraat Water Info*. Accessed: Jan. 2023. [Online]. Available: https://waterinfo.rws.nl/#/nav/index

[4] J. Van Der Jagt, “A methodology for assessing power performance of wave energy converters, applied to a quasi-rigid submerged pressure differential device,” M.S. thesis, Dept. Maritime Mater. Eng., Delft Univ. Technol., Delft, The Netherlands, 2018.

[5] A. Ruezga and J. M. Cañedo C., “Buoy analysis in a point-absorber wave energy converter,” *IEEE J. Ocean. Eng.*, vol. 45, no. 2, pp. 472–479, Apr. 2020.

[6] *Aqwa v2019 R1 Theory Manual*, ANSYS, Canonsburg, PA, USA, 2019.

[7] S. Astariz and G. Iglesias, “Output power smoothing and reduced downtime period by combined wind and wave energy farms,” *Energy*, vol. 97, pp. 69–81, Feb. 2016, doi: 10.1016/j.energy.2015.12.108.

[8] E. Gaertner et al., “Definition of the IEA 15-megawatt offshore ReferenceWind,” Nat. Renew. Energy Lab., Golden, CO, USA, Tech. Rep., NREL/TP-5000-75698, 2020. [Online]. Available: https://www.nrel.gov/docs/fy20osti/75698.pdf